Latin American Journal of Solids and Structures
www.lajss.org

Closed-form Solution for Freely Vibrating Functionally Graded Thick Doubly Curved Panel-A New Generic Approach

Abstract

Today, double curvature shell panels are the main parts of each design because their geometrical characteristics provide high strength to weight ratio, aerodynamic form and beauty for the structures such as boats, submarines, automobiles and buildings. Also, functionally graded materials which present multiple properties such as high mechanical and heat resistant, simultaneously, have attracted designers. So, as the first step of any dynamic analysis, this paper concentrates on presenting a high precision and reliable method for free vibration analysis of functionally graded doubly curved shell panels. To this end, panel is modeled based on third order shear deformation theory and both of the Donnell and Sanders strain-displacement relations. A new set of potential functions and auxiliary variables are proposed to present an exact Levy-type close-form solution for vibrating FG panel. The validity and accuracy of present method are confirmed by comparing results with literature and finite element method. Also, effect of various parameters on natural frequencies are studied which are helpful for designers.

Keywords

Free vibration, exact solution, doubly curved panel, functionally graded material, third order displacement field.

M. Fadaee [a*]
M. R Ilkhani [b]

[a] Department of Mechanical Engineering,College of Engineering,
Qom University of Technology,
Qom 37195-1519, Iran.
[b] Impact Research Laboratory, Department of Mechanical Engineering, Iran University of Science and Technology,
Tehran, Iran.
[*]E-mail: fadaee@qut.ac.ir

http://dx.doi.org/10.1590/1679-78251550

Received 15.09.2014
In Revised Form 20.11.2014
Accepted 21.11.2014
Available online 17.12.2014

1 INTRODUCTION

Growing need of humans to optimal use of material, energy, and time forces engineers to combine multiple useful engineering ideas in their designs. These considerations lead to design of complex structures. One of these ideas is to construct a material with variable properties between its top and bottom layers. The main goal of this invention was to combine heat resistant of ceramic with mechanical strength of steel in order to use in aircraft and spacecraft structures. Also, continuous variation of mechanical properties overcome delamination problems in composites. This material was produced in the national aerospace agency of Japan which is known today as functionally graded material (Hirai et al., 1988). Functionally graded materials (FGMs) are non-homogeneous isotropic,

orthotropic and even anisotropic materials whose mechanical properties vary through one, two or three directions. Applications of these materials in different geometries such as beam, plate, cylinder, cylindrical panels, and doubly curved panels have been investigated in the past years. To this end, various geometrical theories such as Love (1927), Donnell (1934), Sanders (1959), Novozhilov (1959), Flugge (1962), and etc have been used. Also, in order to improve results accuracy, different displacement fields such as classical, first order shear deformation (Mindlin, 1951; Reissner, 1945), and third order shear deformation (Reddy and Liu, 1985) theories have been applied in models. Among the numerous research paper published in this area, papers presented by Wu et al. (1998), Singh (1999), Messina (2003), Chaudhuri et al. (2005), Redekop (2006), Biglari and Jafari (2010), and Fazzolari and Carrera (2013) are examples of papers which studied vibrational behavior of composite structures, especially doubly curved panels. Also, Papers provided by Zahedinejad et al. (2010), Alibeigloo and Chen (2010), Vel (2010), Hashemi et al. (2012), Kiani et al. (Kiani et al., 2012; Kiani et al., 2013), Civalek et al. (Akgöz and Civalek, 2013; Civalek, 2005), Su et al. (2014), and Sayyaadi et al. (2014) are good examples of researches which used various geometrical theories to analyze free vibration of FG structures such as cylindrical and doubly curved panels. These analysis shows that higher order displacement fields gives more accurate results respect to the lower ones but higher ones are computationally expensive. Additionally, Tornabene et al. (Tornabene, 2009, 2011a, b; Tornabene et al., 2014; Tornabene et al., 2012; Tornabene et al., 2013; Viola et al., 2013) have developed generalized differential quadrature (GDQ) to analyzed various FG structures. Furthermore, Zhang and Liew with their coworkers have applied mesh-less methods to analyze different FG shells (Lei et al., 2014; Liew et al., 2014; Liew et al., 2011; Zhang et al., 2014a, b; Zhang et al., 2014c; Zhu et al., 2014).

Our literature survey shows that all related papers used first or third order shear deformation theories. But they either preferred numerical methods such as Rayleigh-Ritz, GDQ, and FE methods or presented Navier's solution for FG doubly curved panels. Indeed, there is no paper which presents exact solution for third order FG doubly curved shell panels. Therefore, in this paper our success in eliminating this defect is presented. In the present paper, a new exact closed-from solution is proposed for freely vibrating functionally graded doubly curved panel. To this end, equations of motion are derived by combining third order shear deformation theory with Donnell and Sanders strain fields. A new set of potential functions which satisfies Levy-type boundary conditions are applied to the equations of motion to decouple partial differential equations. By applying Levy-type boundary conditions to the equations, natural frequencies of FG doubly curved panel are found. Validity and accuracy of the present method are verified by comparing them with literature and finite element results. Also, the effect of different geometrical and material parameters changes on natural frequencies are investigated in various figures.

2 MATHEMATICAL FORMULATIONS

2.1 Material and geometrical assumptions

Consider a doubly curved shallow shell with rectangular base (as shown in Figure 1). A curvilinear coordinate system (x_1, x_2, x_3) is used, with the x_1 and x_2 plane coinciding with the middle surface

of the shell in its initial, undeformed configuration and the x_3 axis normal to it. The principal radii of curvature R_1 and R_2 are assumed to be constant along the shell. a and b are the curvilinear lengths of the edges and h is the shell thickness. The displacements of an arbitrary point of coordinates (x_1, x_2) on the middle surface of the shell are denoted by u, v and w, in the x_1, x_2 and x_3 directions, respectively. The shell has two opposite edges simply supported along x_2 axis (i.e. along the edges $x_1 = 0$ and $x_1 = a$) while the other two edges may be free, simply supported or clamped.

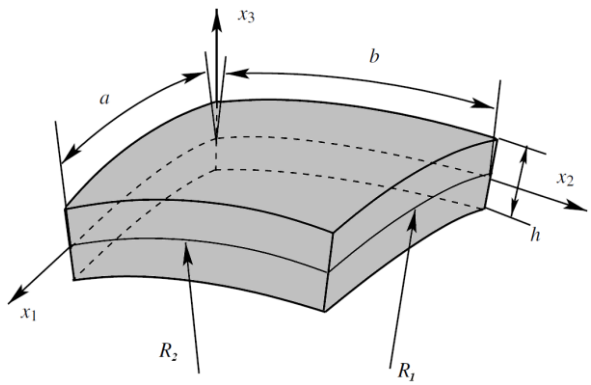

Figure 1: Geometry of a FG doubly curved shell panel

The material properties of the shell are assumed to vary through the thickness according to a power-law distribution of the volume fractions of the two materials as ceramic and metal. Poisson's ratio ν is assumed to be constant and is taken as 0.3. Young's modulus and mass density are assumed to vary continuously through the shell thickness as

$$\begin{aligned} E(x_3) &= (E_c - E_m)V_f(x_3) + E_m, \\ \rho(x_3) &= (\rho_c - \rho_m)V_f(x_3) + \rho_m, \end{aligned} \tag{1}$$

In which the subscripts m and c represent the metallic and ceramic constituents, respectively, and the volume fraction V_f may be given by

$$V_f(x_3) = (\frac{x_3}{h} + \frac{1}{2})^p \tag{2}$$

where p is the power law index and takes only positive values. Typical values for metal and ceramics used in the FG shell are listed in Table 1.

Material	Properties		
	E (GPa)	ν	ρ (Kg/m^3)
Aluminum (Al)	70	0.3	2700
Alumina (Al_2O_3)	380	0.3	3800
Zirconia (ZrO_2)	200	0.3	5700

Table 1: Material properties of the used FG shell.

2.2 Constitutive Relations Based on the TSDT

According to the third order shear deformation shell theories of Donnell and Sanders (TSDT) in which the in-plane displacements are expanded as cubic functions of the thickness coordinate and the transverse deflection is constant through the shell thickness, the displacement field is used as follows (Reddy, 2004)

$$u_1(x_1,x_2,x_3,t)=u(x_1,x_2,t)+x_3\psi_1(x_1,x_2,t)-\frac{4x_3^3}{3h^2}(\psi_1(x_1,x_2,t)+\frac{\partial w(x_1,x_2,t)}{\partial x_1}-c_1\frac{u(x_1,x_2,t)}{R_1}) \tag{3a}$$

$$u_2(x_1,x_2,x_3,t)=v(x_1,x_2,t)+x_3\psi_2(x_1,x_2,t)-\frac{4x_3^3}{3h^2}(\psi_2(x_1,x_2,t)+\frac{\partial w(x_1,x_2,t)}{\partial x_2}-c_1\frac{v(x_1,x_2,t)}{R_2}) \tag{3b}$$

$$u_3(x_1,x_2,x_3,t)=w(x_1,x_2,t) \tag{3c}$$

where ψ_1, ψ_2 denote the rotations of normal to mid-plane about the x_2 and x_1 axes, respectively and t is the time. The strain-displacement relations are given as (Reddy, 2004)

$$\begin{gathered}\varepsilon_1=\varepsilon_1^0+x_3\kappa_1^0+x_3^3\kappa_1^2 \qquad \varepsilon_2=\varepsilon_2^0+x_3\kappa_2^0+x_3^3\kappa_2^2 \qquad \varepsilon_6=\varepsilon_6^0+x_3\kappa_6^0+x_3^3\kappa_6^2 \\ \varepsilon_4=\varepsilon_4^0+x_3^2\kappa_4^1 \qquad \varepsilon_5=\varepsilon_5^0+x_3^2\kappa_5^1\end{gathered} \tag{4}$$

where

$$\begin{gathered}\varepsilon_1^0=\frac{\partial u}{\partial x_1}+\frac{w}{R_1} \qquad \kappa_1^0=\frac{\partial \psi_1}{\partial x_1} \qquad \varepsilon_2^0=\frac{\partial v}{\partial x_2}+\frac{w}{R_2} \\ \kappa_2^0=\frac{\partial \psi_2}{\partial x_2} \qquad \varepsilon_6^0=\frac{\partial u}{\partial x_2}+\frac{\partial v}{\partial x_1} \qquad \kappa_6^0=\frac{\partial \psi_1}{\partial x_2}+\frac{\partial \psi_2}{\partial x_1} \\ \varepsilon_4^0=\frac{\partial w}{\partial x_2}+\psi_2-c_1\frac{v}{R_2} \qquad \varepsilon_5^0=\frac{\partial w}{\partial x_1}+\psi_1-c_1\frac{u}{R_1} \\ \kappa_1^2=-\frac{4}{3h^2}\left(\frac{\partial \psi_1}{\partial x_1}+\frac{\partial^2 w}{\partial x_1^2}-c_1\frac{1}{R_1}\frac{\partial u}{\partial x_1}\right) \qquad \kappa_2^2=-\frac{4}{3h^2}\left(\frac{\partial \psi_2}{\partial x_2}+\frac{\partial^2 w}{\partial x_2^2}-c_1\frac{1}{R_2}\frac{\partial v}{\partial x_2}\right) \\ \kappa_6^2=-\frac{4}{3h^2}\left(\frac{\partial \psi_2}{\partial x_1}+\frac{\partial \psi_1}{\partial x_2}+2\frac{\partial^2 w}{\partial x_1\partial x_2}-c_1\left(\frac{1}{R_2}\frac{\partial v}{\partial x_1}+\frac{1}{R_1}\frac{\partial u}{\partial x_2}\right)\right) \\ \kappa_4^1=-\frac{4}{h^2}\left(\frac{\partial w}{\partial x_2}+\psi_2-c_1\frac{v}{R_2}\right) \qquad \kappa_5^1=-\frac{4}{h^2}\left(\frac{\partial w}{\partial x_1}+\psi_1-c_1\frac{u}{R_1}\right)\end{gathered} \tag{5}$$

where $c_1 = 0$ and $c_1 = 1$ correspond to Donnell and Sanders theories, respectively.
Based on Hooke's law and using Eqs. (3-5), the stress-displacement relations are defined as

$$\begin{Bmatrix}\sigma_1\\ \sigma_2\\ \sigma_6\\ \sigma_4\\ \sigma_5\end{Bmatrix} = \frac{E}{1-\nu^2}\Bigg(\begin{Bmatrix} u_{,1}+\nu v_{,2}+(\frac{1}{R_1}+\frac{\nu}{R_2})w\\ v_{,2}+\nu u_{,1}+(\frac{1}{R_2}+\frac{\nu}{R_1})w\\ \frac{1-\nu}{2}(u_{,2}+v_{,1})\\ \frac{1-\nu}{2}(\psi_2+w_{,2}-c_1\frac{v}{R_2})\\ \frac{1-\nu}{2}(\psi_1+w_{,1}-c_1\frac{u}{R_1})\end{Bmatrix} + x_3\begin{Bmatrix}\psi_{1,1}+\nu\psi_{2,2}\\ \psi_{2,2}+\nu\psi_{1,1}\\ \frac{1-\nu}{2}(\psi_{1,2}+\psi_{2,1})\\ 0\\ 0\end{Bmatrix} - \frac{4x_3^2}{h^2}\begin{Bmatrix}0\\0\\0\\ \frac{1-\nu}{2}(\psi_2+w_{,2}-c_1\frac{v}{R_2})\\ \frac{1-\nu}{2}(\psi_1+w_{,1}-c_1\frac{u}{R_1})\end{Bmatrix}$$
$$-\frac{4x_3^3}{3h^2}\begin{Bmatrix}(\psi_{1,1}+w_{,11}-c_1\frac{1}{R_1}u_{,1})+\nu(\psi_{2,2}+w_{,22}-c_1\frac{1}{R_2}v_{,2})\\ (\psi_{2,2}+w_{,22}-c_1\frac{1}{R_2}v_{,2})+\nu(\psi_{1,1}+w_{,11}-c_1\frac{1}{R_1}u_{,1})\\ \frac{1-\nu}{2}(\psi_{1,2}+\psi_{2,1}+2w_{,12}-c_1(\frac{1}{R_2}v_{,1}+\frac{1}{R_1}u_{,2}))\\ 0\\ 0\end{Bmatrix}\Bigg) \tag{6}$$

where a comma followed by 1 and 2 denotes the differentiation with respect to x_1 and x_2 coordinates.

2.3 Non-dimensional Equations of Motion

Based on Hamilton's principle, the partial differential equations of motion of vibrating FG doubly curved shell panels based on TSDT are calculated by applying part by part integration technique:

$$\frac{\partial N_1}{\partial x_1}+\frac{\partial N_6}{\partial x_2}+\frac{c_1}{R_1}(\bar{Q}_1+\frac{4}{3h^2}(\frac{\partial P_1}{\partial x_1}+\frac{\partial P_6}{\partial x_2})) = \hat{I}_1\ddot{u}+\hat{J}_2\ddot{\psi}_1-\frac{4}{3h^2}\hat{I}_4\frac{\partial\ddot{w}}{\partial x_1} \tag{7a}$$

$$\frac{\partial N_2}{\partial x_2}+\frac{\partial N_6}{\partial x_1}+\frac{c_1}{R_2}(\bar{Q}_2+\frac{4}{3h^2}(\frac{\partial P_2}{\partial x_2}+\frac{\partial P_6}{\partial x_1})) = \hat{I}_{11}\ddot{v}+\hat{J}_{22}\ddot{\psi}_2-\frac{4}{3h^2}\hat{I}_{44}\frac{\partial\ddot{w}}{\partial x_2} \tag{7b}$$

$$\frac{\partial\bar{M}_1}{\partial x_1}+\frac{\partial\bar{M}_6}{\partial x_2}-\bar{Q}_1 = \hat{J}_2\ddot{u}+J_3\ddot{\psi}_1-\frac{4}{3h^2}J_5\frac{\partial\ddot{w}}{\partial x_1} \tag{7c}$$

$$\frac{\partial\bar{M}_2}{\partial x_2}+\frac{\partial\bar{M}_6}{\partial x_1}-\bar{Q}_2 = \hat{J}_{22}\ddot{v}+J_3\ddot{\psi}_2-\frac{4}{3h^2}J_5\frac{\partial\ddot{w}}{\partial x_2} \tag{7d}$$

$$\frac{\partial \bar{Q}_1}{\partial x_1}+\frac{\partial \bar{Q}_2}{\partial x_2}+\frac{4}{3h^2}(\frac{\partial^2 P_1}{\partial x_1^2}+2\frac{\partial^2 P_6}{\partial x_1 \partial x_2}+\frac{\partial^2 P_2}{\partial x_2^2})-\frac{N_1}{R_1}-\frac{N_2}{R_2} \tag{7e}$$
$$= I_1\ddot{w}-(\frac{4}{3h^2})^2 I_7(\frac{\partial^2 \ddot{w}}{\partial x_1^2}+\frac{\partial^2 \ddot{w}}{\partial x_2^2})+\frac{4}{3h^2}(\hat{I}_4\frac{\partial \ddot{u}}{\partial x_1}+\hat{I}_{44}\frac{\partial \ddot{v}}{\partial x_2})+\frac{4}{3h^2}J_5(\frac{\partial \ddot{\psi}_1}{\partial x_1}+\frac{\partial \ddot{\psi}_2}{\partial x_2})$$

where the overdot denotes time derivative. The stress resultants $N_i, \bar{M}_i, P_i\ (i=1,2,6)$, $\bar{Q}_i\ (i=1,2)$ and the inertia as $I_i\ (i=1,7)$, $J_3, J_5, \hat{J}_2, \hat{J}_{22}$, $\hat{I}_i, \hat{I}_{ii}\ (i=1,4)$ are defined as

$$\begin{aligned}
&I_i=\int_{-\frac{h}{2}}^{+\frac{h}{2}}\rho\, x_3^{i-1}\,dx_3 \quad , \qquad (i=1,2,3,4,5,7)\\
&J_i=I_i-\frac{4}{3h^2}I_{i+2} \quad , \quad (i=2,5)\\
&J_3=I_3-\frac{8}{3h^2}I_5+\frac{16}{9h^4}I_7\\
&\hat{I}_1=I_1+c_1(\frac{1}{R_1}\frac{8}{3h^2}I_4+\frac{1}{R_1^2}\frac{16}{9h^4}I_7) \quad , \quad \hat{I}_{11}=I_1+c_1(\frac{1}{R_2}\frac{8}{3h^2}I_4+\frac{1}{R_2^2}\frac{16}{9h^4}I_7)\\
&\hat{J}_2=J_2+c_1(\frac{1}{R_1}\frac{4}{3h^2}J_5) \quad , \quad \hat{J}_{22}=J_2+c_1(\frac{1}{R_2}\frac{4}{3h^2}J_5)\\
&\hat{I}_4=I_4+c_1(\frac{1}{R_1}\frac{4}{3h^2}I_7) \quad , \quad \hat{I}_{44}=I_4+c_1(\frac{1}{R_2}\frac{4}{3h^2}I_7)
\end{aligned} \tag{8}$$

$$N_i, M_i, P_i \ = \int_{-h/2}^{+h/2}\sigma_i\ \ 1, x_3, x_3^3\ dx_3 \quad , \quad i=1,2,6 \tag{9a}$$

$$\bar{M}_i = M_i-\frac{4}{3h^2}P_i \quad , \quad i=1,2,6 \tag{9b}$$

$$Q_2, K_2 \ = \int_{-h/2}^{+h/2}\sigma_4\ \ 1, x_3^2\ dx_3 \tag{9c}$$

$$Q_1, K_1 \ = \int_{-h/2}^{+h/2}\sigma_5\ \ 1, x_3^2\ dx_3 \tag{9d}$$

$$\bar{Q}_i = Q_i-\frac{4}{h^2}K_i \quad , \quad i=1,2 \tag{9e}$$

For brevity, the non-dimensional parameters are introduced as

$$
\begin{aligned}
&X_1 = \frac{x_1}{a}\ ,\ X_2 = \frac{x_2}{a}\ ,\ \eta = \frac{b}{a}\ ,\ \tau = \frac{h}{a}\ ,\ \delta_1 = \frac{R_1}{a}\ ,\ \delta_2 = \frac{R_2}{a}\ ,\ \beta = \omega a^2 / h\sqrt{\rho_c / E_c} \\
&\tilde{u} = \frac{u}{a}\quad ,\quad \tilde{v} = \frac{v}{a}\quad ,\quad \tilde{w} = \frac{w}{a}\quad ,\quad \tilde{\psi}_1 = \psi_1\quad ,\quad \tilde{\psi}_2 = \psi_2 \\
&\bar{I}_1 = \frac{I_1}{\rho_c a}\ ,\ \bar{I}_2 = \frac{I_2}{\rho_c a^2}\ ,\ \bar{I}_3 = \frac{I_3}{\rho_c a^3}\ ,\ \bar{I}_4 = \frac{I_4}{\rho_c a^4}\ ,\ \bar{I}_5 = \frac{I_5}{\rho_c a^5}\ ,\ \bar{I}_7 = \frac{I_7}{\rho_c a^7} \\
&\bar{J}_2 = \frac{J_2}{\rho_c a^2}\ ,\ \bar{J}_3 = \frac{J_3}{\rho_c a^3}\ ,\ \bar{J}_5 = \frac{J_5}{\rho_c a^5}\ ,\ \bar{\hat{I}}_1 = \frac{\hat{I}_1}{\rho_c a}\ ,\ \bar{\hat{I}}_4 = \frac{\hat{I}_4}{\rho_c a^4}\ ,\ \bar{\hat{J}}_2 = \frac{\hat{J}_2}{\rho_c a^2} \\
&\bar{\hat{I}}_{11} = \frac{\hat{I}_{11}}{\rho_c a}\ ,\ \bar{\hat{J}}_{22} = \frac{\hat{J}_{22}}{\rho_c a^2}\ ,\ \bar{\hat{I}}_{44} = \frac{\hat{I}_{44}}{\rho_c a^4}
\end{aligned}
\tag{10}
$$

where ω is the natural frequency of the shell (rad/s).

Assuming that the five coordinates ψ_1, ψ_2, u, v and w vary harmonically with respect to the time variable t (for the free vibration analysis) and using the non-dimensional parameters defined in Eqs. (10), Eqs. (7a-c) can be expressed as

$$
\begin{aligned}
&(\bar{A} + c_1\frac{8(2\bar{H} + 3\bar{G}\delta_1\tau^2)}{9\delta_1^2\tau^4})(\frac{1-\nu}{2}\nabla^2\tilde{u} + \frac{1+\nu}{2}(\tilde{u}_{,1} + \tilde{v}_{,2})_{,1}) \\
&+(\bar{B} - \frac{4}{3\tau^2}\bar{G} + c_1\frac{4(-4\bar{H} + 3\bar{F}\tau^2)}{9\delta_1\tau^4})(\frac{1-\nu}{2}\nabla^2\tilde{\psi}_1 + \frac{1+\nu}{2}(\tilde{\psi}_{1,1} + \tilde{\psi}_{2,2})_{,1}) \\
&+\frac{2c_1(4c_1\bar{H} + 3\bar{G}\delta_1\tau^2)(1+\nu)(\delta_1 - \delta_2)}{9\delta_1^2\delta_2\tau^4}\ \tilde{v}_{,12} + c_1\frac{(-1+\nu)(16\bar{F} - 8\bar{D}\tau^2 + \bar{A}\tau^4)}{2\delta_1^2\tau^4}(\tilde{u} - \delta_1\tilde{\psi}_1) \\
&+\frac{2\delta_1(3\bar{A}(\delta_2 + \delta_1\nu))\tau^4 + c_1(-48\bar{F}\delta_1\delta_2(-1+\nu) + \tau^2(8\bar{G}(\delta_2 + \delta_1\nu) + 3\delta_1\delta_2(-1+\nu)(8\bar{D} - \bar{A}\tau^2)))}{6\delta_1^2\delta_2\tau^4}\ \bar{w}_{,1} \\
&-(\frac{4}{3\tau^2}\bar{G} + c_1\frac{16\bar{H}}{9\delta_1\tau^4})\nabla^2\bar{w}_{,1} = -\bar{\hat{I}}_1\tau^2\beta^2\tilde{u} - \bar{\hat{J}}_2\tau^2\beta^2\tilde{\psi}_1 + \frac{4}{3}\bar{\hat{I}}_4\beta^2\bar{w}_{,1}
\end{aligned}
\tag{11a}
$$

$$
\begin{aligned}
&(\bar{A} + c_1\frac{8(2\bar{H} + 3\bar{G}\delta_1\tau^2)}{9\delta_2^2\tau^4})(\frac{1-\nu}{2}\nabla^2\tilde{v} + \frac{1+\nu}{2}(\tilde{v}_{,2} + \tilde{u}_{,1})_{,2}) \\
&+(\bar{B} - \frac{4}{3\tau^2}\bar{G} + c_1\frac{4(-4\bar{H} + 3\bar{F}\tau^2)}{9\delta_2\tau^4})(\frac{1-\nu}{2}\nabla^2\tilde{\psi}_2 + \frac{1+\nu}{2}(\tilde{\psi}_{2,2} + \tilde{\psi}_{1,1})_{,2}) \\
&-\frac{2c_1(4c_1\bar{H} + 3\bar{G}\delta_2\tau^2)(1+\nu)(\delta_1 - \delta_2)}{9\delta_2^2\delta_1\tau^4}\ \tilde{u}_{,12} + c_1\frac{(-1+\nu)(16\bar{F} - 8\bar{D}\tau^2 + \bar{A}\tau^4)}{2\delta_2^2\tau^4}(\tilde{v} - \delta_2\tilde{\psi}_2) \\
&+\frac{2\delta_2(3\bar{A}(\delta_1 + \delta_2\nu))\tau^4 + c_1(-48\bar{F}\delta_1\delta_2(-1+\nu) + \tau^2(8\bar{G}(\delta_1 + \delta_2\nu) + 3\delta_1\delta_2(-1+\nu)(8\bar{D} - \bar{A}\tau^2)))}{6\delta_2^2\delta_1\tau^4}\ \bar{w}_{,2} \\
&-(\frac{4}{3\tau^2}\bar{G} + c_1\frac{16\bar{H}}{9\delta_2\tau^4})\nabla^2\bar{w}_{,2} = -\bar{\hat{I}}_{11}\tau^2\beta^2\tilde{v} - \bar{\hat{J}}_{22}\tau^2\beta^2\tilde{\psi}_2 + \frac{4}{3}\bar{\hat{I}}_{44}\beta^2\bar{w}_{,2}
\end{aligned}
\tag{11b}
$$

$$
\begin{aligned}
&(\bar{B}-\frac{4}{3\tau^2}\bar{G}+c_1\frac{4(-4\bar{H}+3\bar{F}\tau^2)}{9\delta_1\tau^4})(\frac{1-\nu}{2}\nabla^2\tilde{u}+\frac{1+\nu}{2}(\tilde{u}_{,1}+\tilde{v}_{,2})_{,1})\\
&+(\bar{D}+\frac{8(2\bar{H}-3\bar{F}\tau^2)}{9\tau^4})(\frac{1-\nu}{2}\nabla^2\tilde{\psi}_1+\frac{1+\nu}{2}(\tilde{\psi}_{1,1}+\tilde{\psi}_{2,2})_{,1})\\
&+\frac{2c_1(4\bar{H}-3\bar{F}\tau^2)(1+\nu)(\delta_1-\delta_2)}{9\delta_1\delta_2\tau^4}\tilde{v}_{,12}-c_1\frac{(-1+\nu)(16\bar{F}-8\bar{D}\tau^2+\bar{A}\tau^4)}{2\delta_1\tau^4}(\tilde{u}-\frac{\delta_1}{c_1}\tilde{\psi}_1)\\
&+\frac{48\bar{F}\delta_1\delta_2(-1+\nu)+\tau^2(-24\delta_1\delta_2\bar{D}(-1+\nu)-8\bar{G}(\delta_2+\delta_1\nu)+(\delta_1\delta_2(3\bar{A}(-1+\nu))+6\bar{B}(\delta_2+\delta_1\nu))\tau^2)}{6\delta_1\delta_2\tau^4}\bar{w}_{,1}\\
&+(\frac{16\bar{H}}{9\tau^4}-\frac{4\bar{F}}{3\tau^2})\nabla^2\bar{w}_{,1}=-\bar{\bar{J}}_2\tau^2\beta^2\tilde{u}-\bar{J}_3\tau^2\beta^2\tilde{\psi}_1+\frac{4}{3}\bar{J}_5\beta^2\bar{w}_{,1}
\end{aligned}
\tag{11c}
$$

$$
\begin{aligned}
&(\bar{B}-\frac{4}{3\tau^2}\bar{G}+c_1\frac{4(-4\bar{H}+3\bar{F}\tau^2)}{9\delta_2\tau^4})(\frac{1-\nu}{2}\nabla^2\tilde{v}+\frac{1+\nu}{2}(\tilde{v}_{,2}+\tilde{u}_{,1})_{,2})\\
&+(\bar{D}+\frac{8(2\bar{H}-3\bar{F}\tau^2)}{9\tau^4})(\frac{1-\nu}{2}\nabla^2\tilde{\psi}_2+\frac{1+\nu}{2}(\tilde{\psi}_{2,2}+\tilde{\psi}_{1,1})_{,2})\\
&-\frac{2c_1(4\bar{H}-3\bar{F}\tau^2)(1+\nu)(\delta_1-\delta_2)}{9\delta_1\delta_2\tau^4}\tilde{u}_{,12}-c_1\frac{(-1+\nu)(16\bar{F}-8\bar{D}\tau^2+\bar{A}\tau^4)}{2\delta_2\tau^4}(\tilde{v}-\frac{\delta_2}{c_1}\tilde{\psi}_2)\\
&+\frac{48\bar{F}\delta_1\delta_2(-1+\nu)+\tau^2(-24\delta_1\delta_2\bar{D}(-1+\nu)-8\bar{G}(\delta_1+\delta_2\nu)+(\delta_1\delta_2(3\bar{A}(-1+\nu))+6\bar{B}(\delta_1+\delta_2\nu))\tau^2)}{6\delta_1\delta_2\tau^4}\bar{w}_{,2}\\
&+(\frac{16\bar{H}}{9\tau^4}-\frac{4\bar{F}}{3\tau^2})\nabla^2\bar{w}_{,2}=-\bar{\bar{J}}_{22}\tau^2\beta^2\tilde{v}-\bar{J}_3\tau^2\beta^2\tilde{\psi}_2+\frac{4}{3}\bar{J}_5\beta^2\bar{w}_{,2}
\end{aligned}
\tag{11d}
$$

$$
\begin{aligned}
&(\frac{4\bar{F}}{3\tau^2}-\frac{16\bar{H}}{9\tau^4})\nabla^2(\tilde{\psi}_{1,1}+\tilde{\psi}_{2,2})-\frac{16\bar{H}}{9\tau^4}\nabla^4\tilde{w}-(\frac{\bar{A}}{\delta_1^2}+\frac{\bar{A}}{\delta_2^2}+\frac{2\bar{A}\nu}{\delta_1\delta_2})\tilde{w}\\
&+\frac{-144\bar{F}\delta_1\delta_2(-1+\nu)+\tau^2(48\bar{G}(\delta_2+\delta_1\nu)+\delta_1\delta_2(-1+\nu)(72\bar{D}-9\bar{A}\tau^2))}{18\delta_1\delta_2\tau^4}\tilde{w}_{,11}\\
&+\frac{-144\bar{F}\delta_1\delta_2(-1+\nu)+\tau^2(48\bar{G}(\delta_1+\delta_2\nu)+\delta_1\delta_2(-1+\nu)(72\bar{D}-9\bar{A}\tau^2))}{18\delta_1\delta_2\tau^4}\tilde{w}_{,22}\\
&+(\frac{4\bar{G}}{3\tau^2}+c_1\frac{16\bar{H}}{9\delta_1\tau^4})\nabla^2(\tilde{u}_{,1})+(\frac{4\bar{G}}{3\tau^2}+c_1\frac{16\bar{H}}{9\delta_2\tau^4})\nabla^2(\tilde{v}_{,2})\\
&+\frac{-48\bar{F}\delta_1\delta_2(-1+\nu)+\tau^2(24\bar{D}\delta_1\delta_2(-1+\nu)+8\bar{G}(\delta_2+\delta_1\nu)+(\delta_1\delta_2(3\bar{A}-3\bar{A}\nu)-6\bar{B}(\delta_2+\delta_1\nu))\tau^2)}{6\delta_2\delta_1\tau^4}\tilde{\psi}_{1,1}\\
&+\frac{-48\bar{F}\delta_1\delta_2(-1+\nu)+\tau^2(24\bar{D}\delta_1\delta_2(-1+\nu)+8\bar{G}(\delta_1+\delta_2\nu)+(\delta_1\delta_2(3\bar{A}-3\bar{A}\nu)-6\bar{B}(\delta_1+\delta_2\nu))\tau^2)}{6\delta_2\delta_1\tau^4}\tilde{\psi}_{2,2}\\
&+\frac{-2\delta_2(3\bar{A}(\delta_1+\delta_2\nu))\tau^4+c_1(48\bar{F}\delta_1\delta_2(-1+\nu)+\tau^2(-8\bar{G}(\delta_1+\delta_2\nu)-3\delta_1\delta_2(-1+\nu)(8\bar{D}-\bar{A}\tau^2)))}{6\delta_2^2\delta_1\tau^4}\tilde{v}_{,2}\\
&+\frac{-2\delta_1(3\bar{A}(\delta_2+\delta_1\nu))\tau^4+c_1(48\bar{F}\delta_1\delta_2(-1+\nu)+\tau^2(-8\bar{G}(\delta_2+\delta_1\nu)-3\delta_1\delta_2(-1+\nu)(8\bar{D}-\bar{A}\tau^2)))}{6\delta_1^2\delta_2\tau^4}\tilde{u}_{,1}\\
&=-\bar{I}_1\tau^2\beta^2\tilde{w}+\frac{16}{9\tau^2}\bar{I}_7\beta^2\nabla^2\tilde{w}-\frac{4}{3}\beta^2(\bar{\bar{I}}_4\tilde{u}_{,1}+\bar{\bar{I}}_{44}\tilde{v}_{,2})-\frac{4}{3}\bar{J}_5\beta^2(\tilde{\psi}_{1,1}+\tilde{\psi}_{2,2})
\end{aligned}
\tag{11e}
$$

where

$$\nabla^2 = \frac{\partial^2}{\partial X_1^2} + \frac{\partial^2}{\partial X_2^2} \tag{12}$$
$$\nabla^4 = \frac{\partial^4}{\partial X_1^4} + 2\frac{\partial^4}{\partial X_1^2 \partial X_2^2} + \frac{\partial^4}{\partial X_2^4}$$

And

$$(A,B,D,G,F,H) = \int_{-h/2}^{h/2} \frac{E(x_3)}{1-\nu^2}(1, x_3, x_3^2, x_3^3, x_3^4, x_3^6)\, dx_3 \tag{13a}$$

$$\bar{A} = \frac{A}{E_c a} \quad , \quad \bar{B} = \frac{B}{E_c a^2} \quad , \quad \bar{D} = \frac{D}{E_c a^3} \quad , \quad \bar{G} = \frac{G}{E_c a^4} \quad , \quad \bar{F} = \frac{F}{E_c a^5} \quad , \quad \bar{H} = \frac{H}{E_c a^7} \tag{13b}$$

2.4 Exact Solution Procedure

The eight auxiliary functions f_1, f_2, f_3, f_4 and $\varphi_1, \varphi_2, \varphi_3, \varphi_4$ are introduced as

$$f_1 = \left(\bar{A} + c_1 \frac{8\ 2\bar{H} + 3\bar{G}\delta_1\tau^2}{9\delta_1^2\tau^4}\right)\frac{1-\nu}{2}\tilde{u} + \left(\bar{B} - \frac{4}{3\tau^2}\bar{G} + c_1 \frac{4\ -4\bar{H} + 3\bar{F}\tau^2}{9\delta_1\tau^4}\right)\frac{1-\nu}{2}\tilde{\psi}_1 \tag{14a}$$

$$f_2 = \left(\bar{A} + c_1 \frac{8\ 2\bar{H} + 3\bar{G}\delta_2\tau^2}{9\delta_2^2\tau^4}\right)\frac{1-\nu}{2}\tilde{v} + \left(\bar{B} - \frac{4}{3\tau^2}\bar{G} + c_1 \frac{4\ -4\bar{H} + 3\bar{F}\tau^2}{9\delta_2\tau^4}\right)\frac{1-\nu}{2}\tilde{\psi}_2 \tag{14b}$$

$$f_3 = \left(\bar{B} - \frac{4}{3\tau^2}\bar{G} + c_1 \frac{4\ -4\bar{H} + 3\bar{F}\tau^2}{9\delta_1\tau^4}\right)\frac{1-\nu}{2}\tilde{u} + \left(\bar{D} - \frac{8}{3\tau^2}\bar{F} + \frac{16}{9\tau^4}\bar{H}\right)\frac{1-\nu}{2}\tilde{\psi}_1 \tag{14c}$$

$$f_4 = \left(\bar{B} - \frac{4}{3\tau^2}\bar{G} + c_1 \frac{4\ -4\bar{H} + 3\bar{F}\tau^2}{9\delta_2\tau^4}\right)\frac{1-\nu}{2}\tilde{v} + \left(\bar{D} - \frac{8}{3\tau^2}\bar{F} + \frac{16}{9\tau^4}\bar{H}\right)\frac{1-\nu}{2}\tilde{\psi}_2 \tag{14d}$$

$$\varphi_1 = f_{1,1} + f_{2,2} \tag{15a}$$

$$\varphi_2 = f_{3,1} + f_{4,2} \tag{15b}$$

$$\varphi_3 = f_{1,1} / \delta_1 + f_{2,2} / \delta_2 \tag{15c}$$

$$\varphi_4 = f_{3,1} / \delta_1 + f_{4,2} / \delta_2 \tag{15d}$$

Using these auxiliary functions, the equations of motion of Eqs. (11a-e) may now be expressed as

$$\nabla^2 f_1 + \frac{1+\nu}{1-\nu}\phi_{1,1} = y_1 f_1 + y_2 f_3 + y_3 \tilde{w}_{,1} + y_4 \nabla^2 \tilde{w}_{,1} \tag{16a}$$

$$\nabla^2 f_2 + \frac{1+\nu}{1-\nu}\phi_{1,2} = y_5 f_2 + y_6 f_4 + y_7 \tilde{w}_{,2} + y_8 \nabla^2 \tilde{w}_{,2} \tag{16b}$$

$$\nabla^2 f_3 + \frac{1+\nu}{1-\nu}\phi_{2,1} = y_9 f_1 + y_{10} f_3 + y_{11} \tilde{w}_{,1} + y_{12} \nabla^2 \tilde{w}_{,1} \tag{16c}$$

$$\nabla^2 f_4 + \frac{1+\nu}{1-\nu}\phi_{2,2} = y_{13} f_2 + y_{14} f_4 + y_{15} \tilde{w}_{,2} + y_{16} \nabla^2 \tilde{w}_{,2} \tag{16d}$$

$$\begin{aligned} &y_{17}\nabla^2\phi_1 + y_{18}\nabla^2\phi_2 + y_{19}\nabla^2\phi_3 + y_{20}\nabla^2\phi_4 + y_{21}\phi_1 + y_{22}\phi_2 + y_{23}\phi_3 + y_{24}\phi_4 \\ &\quad = y_{25}\nabla^4\tilde{w} + y_{26}\tilde{w}_{,11} + y_{27}\tilde{w}_{,22} + y_{28}\tilde{w} \end{aligned} \tag{16e}$$

where $y_i\,(i = 1-28)$ are constants governed easily by material properties, non-dimensional frequency β and structural geometry.

2.4.1 Obtaining of $\tilde{w}$

Elimination of f_1, f_2, f_3, f_4 and then $\varphi_1, \varphi_2, \varphi_3, \varphi_4$ between Eqs. (16a-e) and simplifying terms, the following equation is obtained

$$\begin{aligned} &a_1 D_1^{12}\tilde{w} + a_2 D_2^{12}\tilde{w} + a_3 D_1^2 D_2^{10}\tilde{w} + a_4 D_1^{10} D_2^2 \tilde{w} + a_5 D_1^4 D_2^8 \tilde{w} + a_6 D_1^8 D_2^4 \tilde{w} + a_7 D_1^6 D_2^6 \tilde{w} + \ldots \\ &a_8 D_1^{10}\tilde{w} + a_9 D_2^{10}\tilde{w} + a_{10} D_1^2 D_2^8 \tilde{w} + a_{11} D_1^8 D_2^2 \tilde{w} + a_{12} D_1^4 D_2^6 \tilde{w} + a_{13} D_1^6 D_2^4 \tilde{w} + \ldots \\ &a_{14} D_1^8 \tilde{w} + a_{15} D_2^8 \tilde{w} + a_{16} D_1^2 D_2^6 \tilde{w} + a_{17} D_1^6 D_2^2 \tilde{w} + a_{18} D_1^4 D_2^4 \tilde{w} + \ldots \\ &a_{19} D_1^6 \tilde{w} + a_{20} D_2^6 \tilde{w} + a_{21} D_1^2 D_2^4 \tilde{w} + a_{22} D_1^4 D_2^2 \tilde{w} + \ldots \\ &a_{23} D_1^4 \tilde{w} + a_{24} D_2^4 \tilde{w} + a_{25} D_1^2 D_2^2 \tilde{w} + \ldots \\ &a_{26} D_1^2 \tilde{w} + a_{27} D_2^2 \tilde{w} + a_{28}\tilde{w} = 0 \end{aligned} \tag{17}$$

where

$$D_1^2 D_2^4 \tilde{w} = \tilde{w}_{,112222} \tag{18}$$

and $a_i\,(i = 1,2,3,\ldots,27,28)$ are constants and will not be expressed due to the space limits.

Since the Levy-type FG doubly curved shell panel will be used to analyze the free vibration of the shell, the displacement components $(\tilde{u},\tilde{v},\tilde{w},\tilde{\psi}_1,\tilde{\psi}_2)$ will be represented as

$$\tilde{u} = \tilde{u}(X_2)\sin(\xi X_1) \tag{19a}$$

$$\tilde{v} = \tilde{v}(X_2)\cos(\xi X_1) \tag{19b}$$

$$\tilde{\psi}_1 = \tilde{\psi}_1(X_2)\sin(\xi X_1) \tag{19c}$$

$$\tilde{\psi}_2 = \tilde{\psi}_2(X_2)\cos(\xi X_1) \tag{19d}$$

$$\tilde{w} = \tilde{w}(X_2)\sin(\xi X_1) \tag{19e}$$

where

$$\xi = m\pi \qquad , \qquad m = 0,1,2,3,..... \tag{20}$$

Substituting Eq. (19e) into Eq. (17) gives

$$\tilde{w}(X_2) = W_1 + W_2 + W_3 + W_4 + W_5 + W_6 \tag{21}$$

where the W_1, W_2, W_3, W_4, W_5 and W_6 are defined as

$$D_2^2 W_1 + \alpha_1^2 W_1 = 0 \tag{22a}$$

$$D_2^2 W_2 + \alpha_2^2 W_2 = 0 \tag{22b}$$

$$D_2^2 W_3 + \alpha_3^2 W_3 = 0 \tag{22c}$$

$$D_2^2 W_4 + \alpha_4^2 W_4 = 0 \tag{22d}$$

$$D_2^2 W_5 + \alpha_5^2 W_5 = 0 \tag{22e}$$

$$D_2^2 W_6 + \alpha_6^2 W_6 = 0 \tag{22f}$$

and α_1^2, α_2^2, α_3^2, α_4^2, α_5^2 and α_6^2 are the roots of the following sixth-order equation

$$b_1 z^6 + b_2 z^5 + b_3 z^4 + b_4 z^3 + b_5 z^2 + b_6 z + b_7 = 0 \tag{23}$$

The coefficients $b_i\,(i = 1,2,3,4,5,6,7)$ are given as

$$
\begin{aligned}
&b_1 = a_2 \ , \ b_2 = a_9 - \xi^2 a_3 \ , \ b_3 = a_{15} - \xi^2 a_{10} + \xi^4 a_5 \\
&b_4 = a_{20} - \xi^2 a_{16} + \xi^4 a_{12} - \xi^6 a_7 \ , \ b_5 = a_{24} - \xi^2 a_{21} + \xi^4 a_{18} - \xi^6 a_{13} + \xi^8 a_6 \\
&b_6 = a_{27} - \xi^2 a_{25} + \xi^4 a_{22} - \xi^6 a_{17} + \xi^8 a_{11} - \xi^{10} a_4 \\
&b_7 = a_{28} - \xi^2 a_{26} + \xi^4 a_{23} - \xi^6 a_{19} + \xi^8 a_{14} - \xi^{10} a_8 + \xi^{12} a_1
\end{aligned} \tag{24}
$$

Using of Eqs. (16a-e), the introduced functions $\varphi_1, \varphi_2, \varphi_3, \varphi_4$ can be given by

$$
\begin{aligned}
\varphi_1 = {} & d_1 D_1^{10}\tilde{w} + d_2 D_2^{10}\tilde{w} + d_3 D_1^2 D_2^8 \tilde{w} + d_4 D_1^8 D_2^2 \tilde{w} + d_5 D_1^4 D_2^6 \tilde{w} + d_6 D_1^6 D_2^4 \tilde{w} + \ldots \\
& d_7 D_1^8 \tilde{w} + d_8 D_2^8 \tilde{w} + d_9 D_1^2 D_2^6 \tilde{w} + d_{10} D_1^6 D_2^2 \tilde{w} + d_{11} D_1^4 D_2^4 \tilde{w} + \ldots \\
& d_{12} D_1^6 \tilde{w} + d_{13} D_2^6 \tilde{w} + d_{14} D_1^2 D_2^4 \tilde{w} + d_{15} D_1^4 D_2^2 \tilde{w} + \ldots \\
& d_{16} D_1^4 \tilde{w} + d_{17} D_2^4 \tilde{w} + d_{18} D_1^2 D_2^2 \tilde{w} + \ldots \\
& d_{19} D_1^2 \tilde{w} + d_{20} D_2^2 \tilde{w} + d_{21} \tilde{w}
\end{aligned} \tag{25a}
$$

$$
\begin{aligned}
\varphi_2 = {} & e_1 D_1^{10}\tilde{w} + e_2 D_2^{10}\tilde{w} + e_3 D_1^2 D_2^8 \tilde{w} + e_4 D_1^8 D_2^2 \tilde{w} + e_5 D_1^4 D_2^6 \tilde{w} + e_6 D_1^6 D_2^4 \tilde{w} + \ldots \\
& e_7 D_1^8 \tilde{w} + e_8 D_2^8 \tilde{w} + e_9 D_1^2 D_2^6 \tilde{w} + e_{10} D_1^6 D_2^2 \tilde{w} + e_{11} D_1^4 D_2^4 \tilde{w} + \ldots \\
& e_{12} D_1^6 \tilde{w} + e_{13} D_2^6 \tilde{w} + e_{14} D_1^2 D_2^4 \tilde{w} + e_{15} D_1^4 D_2^2 \tilde{w} + \ldots \\
& e_{16} D_1^4 \tilde{w} + e_{17} D_2^4 \tilde{w} + e_{18} D_1^2 D_2^2 \tilde{w} + \ldots \\
& e_{19} D_1^2 \tilde{w} + e_{20} D_2^2 \tilde{w} + e_{21} \tilde{w}
\end{aligned} \tag{25b}
$$

$$
\begin{aligned}
\varphi_3 = {} & g_1 D_1^{10}\tilde{w} + g_2 D_2^{10}\tilde{w} + g_3 D_1^2 D_2^8 \tilde{w} + g_4 D_1^8 D_2^2 \tilde{w} + g_5 D_1^4 D_2^6 \tilde{w} + g_6 D_1^6 D_2^4 \tilde{w} + \ldots \\
& g_7 D_1^8 \tilde{w} + g_8 D_2^8 \tilde{w} + g_9 D_1^2 D_2^6 \tilde{w} + g_{10} D_1^6 D_2^2 \tilde{w} + g_{11} D_1^4 D_2^4 \tilde{w} + \ldots \\
& g_{12} D_1^6 \tilde{w} + g_{13} D_2^6 \tilde{w} + g_{14} D_1^2 D_2^4 \tilde{w} + g_{15} D_1^4 D_2^2 \tilde{w} + \ldots \\
& g_{16} D_1^4 \tilde{w} + g_{17} D_2^4 \tilde{w} + g_{18} D_1^2 D_2^2 \tilde{w} + \ldots \\
& g_{19} D_1^2 \tilde{w} + g_{20} D_2^2 \tilde{w} + g_{21} \tilde{w}
\end{aligned} \tag{25c}
$$

$$
\begin{aligned}
\varphi_4 = {} & h_1 D_1^{10}\tilde{w} + h_2 D_2^{10}\tilde{w} + h_3 D_1^2 D_2^8 \tilde{w} + h_4 D_1^8 D_2^2 \tilde{w} + h_5 D_1^4 D_2^6 \tilde{w} + h_6 D_1^6 D_2^4 \tilde{w} + \ldots \\
& h_7 D_1^8 \tilde{w} + h_8 D_2^8 \tilde{w} + h_9 D_1^2 D_2^6 \tilde{w} + h_{10} D_1^6 D_2^2 \tilde{w} + h_{11} D_1^4 D_2^4 \tilde{w} + \ldots \\
& h_{12} D_1^6 \tilde{w} + h_{13} D_2^6 \tilde{w} + h_{14} D_1^2 D_2^4 \tilde{w} + h_{15} D_1^4 D_2^2 \tilde{w} + \ldots \\
& h_{16} D_1^4 \tilde{w} + h_{17} D_2^4 \tilde{w} + h_{18} D_1^2 D_2^2 \tilde{w} + \ldots \\
& h_{19} D_1^2 \tilde{w} + h_{20} D_2^2 \tilde{w} + h_{21} \tilde{w}
\end{aligned} \tag{25d}
$$

where the constants of $d_i, e_i, g_i, h_i, \quad i = (1,2,3,\ldots,20,21)$ can be obtained using Eqs. (16a-e).

2.4.2 Solution of $\tilde{u}$, $\tilde{v}$, $\tilde{\psi}_1$ and $\tilde{\psi}_2$

Substituting Eqs. (19a-e), (21), (22a-e) and (25a-d) into Eqs. (16a-e), the auxiliary functions f_1, f_2, f_3 and f_4 may be then expressed as

$$f_1 = \left[C_1 W_1 + C_2 W_2 + C_3 W_3 + C_4 W_4 + C_5 W_5 + C_6 W_6\right] sin(\xi X_1) \tag{26a}$$

$$f_2 = \left[C_7 W_{1,2} + C_8 W_{2,2} + C_9 W_{3,2} + C_{10} W_{4,2} + C_{11} W_{5,2} + C_{12} W_{6,2}\right] cos(\xi X_1) \tag{26b}$$

$$f_3 = \left[C_{13} W_1 + C_{14} W_2 + C_{15} W_3 + C_{16} W_4 + C_{17} W_5 + C_{18} W_6\right] sin(\xi X_1) \tag{26c}$$

$$f_4 = \left[C_{19} W_{1,2} + C_{20} W_{2,2} + C_{21} W_{3,2} + C_{22} W_{4,2} + C_{23} W_{5,2} + C_{24} W_{6,2}\right] cos(\xi X_1) \tag{26d}$$

where the coefficients of $C_i (i = 1,2,3,...,23,24)$ may be derived by submitting Eqs. (26a-d) into Eqs. (16a-d) as well as using Eqs. (22a-e).
Finally, the exact closed-form displacement field of the shell according to the TSDT is obtained by substituting Eqs. (26a-d) into Eqs. (14a-d).

2.4.3 Solution of W_1, W_2, W_3, W_4, W_5 and W_6

According to Eqs. (22a-e), the solutions for the $W_i (i = 1,2,3,4,5,6)$ can be written as

$$W_1 = A_1 \sinh(\mu_1 X_2) + A_2 \cosh(\mu_1 X_2) \tag{27a}$$

$$W_2 = A_3 \sinh(\mu_2 X_2) + A_4 \cosh(\mu_2 X_2) \tag{27b}$$

$$W_3 = A_5 \sin(\mu_3 X_2) + A_6 \cos(\mu_3 X_2) \tag{27c}$$

$$W_4 = A_7 \sinh(\mu_4 X_2) + A_8 \cosh(\mu_4 X_2) \tag{27d}$$

$$W_5 = A_9 \sinh(\mu_5 X_2) + A_{10} \cosh(\mu_5 X_2) \tag{27e}$$

$$W_6 = A_{11} \sinh(\mu_6 X_2) + A_{12} \cosh(\mu_6 X_2) \tag{27f}$$

Where

$$\begin{aligned}
\mu_1 &= \left|\sqrt{\alpha_1^2}\right| && \alpha_1^2 < 0 \\
\mu_2 &= \left|\sqrt{\alpha_2^2}\right| && \alpha_2^2 < 0 \\
\mu_3 &= \left|\sqrt{\alpha_3^2}\right| && \alpha_3^2 > 0 \\
\mu_4 &= \left|\sqrt{\alpha_4^2}\right| && \alpha_4^2 < 0 \\
\mu_5 &= \left|\sqrt{\alpha_5^2}\right| && \alpha_5^2 < 0 \\
\mu_6 &= \left|\sqrt{\alpha_6^2}\right| && \alpha_6^2 < 0
\end{aligned} \tag{28}$$

2.5 The Classical Boundary Conditions

The classical boundary conditions of the TSDT may be obtained for an edge parallel to, for example, X_1-axis as

Simply Supported

$$\tilde{u} = 0 \qquad \tilde{N}_2 + 4c_1 / (3\tau^2\delta_2)\tilde{P}_2 = 0 \qquad \tilde{w} = 0 \qquad \tilde{\psi}_1 = 0 \qquad \tilde{M}_2 = 0 \qquad \tilde{P}_2 = 0 \tag{29a}$$

Clamped

$$\tilde{u} = 0 \qquad \tilde{v} = 0 \qquad \tilde{w} = 0 \qquad \tilde{\psi}_1 = 0 \qquad \tilde{\psi}_2 = 0 \qquad \tilde{w}_{,2} = 0 \tag{29b}$$

Free

$$\begin{gathered}
\tilde{N}_2 + 4c_1 / (3\tau^2\delta_2)\tilde{P}_2 = 0 \qquad \tilde{N}_6 + 4c_1 / (3\tau^2\delta_2)\tilde{P}_6 = 0 \qquad \tilde{M}_6 - 4 / (3\tau^2)\tilde{P}_6 = 0 \\
\tilde{M}_2 = 0 \qquad\qquad \tilde{P}_2 = 0 \\
\tilde{Q}_2 - \frac{4}{\tau^2}\tilde{K}_2 + \frac{4}{3\tau^2}(2\frac{\partial \tilde{P}_6}{\partial X_1} + \frac{\partial \tilde{P}_2}{\partial X_2}) + \frac{4}{3}\bar{I}_4\beta^2\tilde{v} + \frac{4}{3}\beta^2\bar{I}_5\tilde{\psi}_2 - \frac{16}{9\tau^2}\beta^2\bar{I}_7(\frac{\partial \tilde{w}}{\partial X_2} + \tilde{\psi}_2 - \frac{c_1}{\delta_2}\tilde{v}) =
\end{gathered} \tag{29c}$$

By changing subscripts 1 and 2 in Eqs.(29a-c), the different boundary conditions are obtained for the edges $X_1 = 0$ and $X_1 = 1$. The present solution procedure has been applied in our previous paper for other geometry which can help researchers in understanding and developing this method (Hosseini-Hashemi and Fadaee, 2011).

3 RESULTS AND DISCUSSION

3.1 Comparison study

In this section, in order to confirm validity and accuracy of present method two tables are presented, firstly. Next, effect of geometrical parameters changes on natural frequencies are studied in various plots. Material properties used in the tables and figures are indicated in table 1. It should be mentioned that in tables natural frequencies are compared with traditional finite element software results. In this case, panels are modeled by dividing its cross section to subsections with constant properties, firstly. Number of layers depends on the thickness and material power index. Next, models are meshed by using a 3D brick element containing 20 nodes with three degree of freedom in each node. Convergency analysis is done by increasing number of layers and number of elements. Finally, optimum number of elements is selected for the analysis.

The accuracy of Donnell and Sanders models are indicated as a percentage as follow:

$$\%Diff = \frac{\text{[FEM[3D] - Present]}}{\text{FEM[3D]}} \times 100 \tag{30}$$

Also, for simplicity the letters S, C and F are used as symbols of simply, clamped and free boundary conditions, respectively.

First six natural frequencies of FG cylindrical shell panel are tabulated in table 2 for different thickness ratios as $\tau = 0.075, 0.1, 0.125$. Donnell, Sanders and FEM methods are used to compute frequencies under SCSC boundary conditions.

$\tau = h/a$	Method	Mode sequence					
		1	2	3	4	5	6
0.075	Present (TSDTD)*	1588.7	2679.6	3508.5	4540.6	4903.4	6052.7
	Present (TSDTS)**	1583.2	2675.3	3503.1	4524.6	4874.1	6048.9
	FEM (3D)	1580.9	2673.6	3501.2	4520.1	4869.7	6043.1
	Diff (%) (TSDTD)	*-0.493*	*-0.224*	*-0.208*	*-0.453*	*-0.692*	*-0.159*
	Diff (%) (TSDTS)	*-0.145*	*-0.064*	*-0.054*	*-0.099*	*-0.090*	*-0.096*
0.1	Present (TSDTD)	1970.2	3422.5	4353.4	5664.7	6170.0	7402.8
	Present (TSDTS)	1965.1	3414.2	4345.5	5641.8	6128.0	7397.7
	FEM (3D)	1962.2	3412.0	4340.1	5640.1	6122.1	7390.1
	Diff (%) (TSDTD)	*-0.408*	*-0.308*	*-0.306*	*-0.436*	*-0.782*	*-0.172*
	Diff (%) (TSDTS)	*-0.148*	*-0.064*	*-0.124*	*-0.030*	*-0.096*	*-0.103*
0.125	Present (TSDTD)	2328.8	4160.6	5079.2	6607.2	7241.5	8476.6
	Present (TSDTS)	2318.7	4123.9	5068.9	6577.3	7187.4	8470.6
	FEM (3D)	2313.3	4061.3	5061.2	6570.0	7180.1	8463.2
	Diff (%) (TSDTD)	*-0.670*	*-2.445*	*-0.356*	*-0.566*	*-0.855*	*-0.158*
	Diff (%) (TSDTS)	*-0.233*	*-1.541*	*-0.152*	*-0.111*	*-0.102*	*-0.087*

Table 2: Comparison of first six natural frequencies (Hz) for SCSC functionally graded (Al/Al_2O_3)

cylindrical shell panels ($\delta_1 = 6/\pi$, $\delta_2 = \infty$, $\eta = 1$, $R_1 = 1(m)$, $p = 1$). *Donnell third order shear deformation theory; **Sanders third order shear deformation theory

According to table 2, the present method captures natural frequencies, precisely. Also, both of the Donnell and Sanders theories have good agreement with the finite element results but Sanders one is more accurate than Donnell one. It is because of curvature which is considered in the strain relations in the Sanders theory. Furthermore, table 2 shows that increasing the thickness ratio τ increases the natural frequencies. Increasing the panel rigidity is the main reason of such behavior.

As another comparison, in table 3, fundamental natural frequency parameters $\bar{\bar{\beta}}$ of a simply-supported doubly curved FG panel are compared with literature (Farid et al., 2010) for different deep ratio $\delta_1 = 5,10$ and power index p. panel geometrical properties are considered as $\tau = 0.1$, $\eta = 1$, $\delta_2 = \infty$, $D_m = E_m h^3 / (12(1-\nu^2))$. Reference (Farid et al., 2010) solved three dimensional model of FG doubly curved panel by using differential quadrature method. Table 3 confirms validity and accuracy of present method for computing FG doubly curved panel frequencies. Additionally, table 3 shows that increasing power law index reduces natural frequencies. This behavior depends on the arrangement of inner and outer materials of the panel. For table 3 aluminum/alumina composition is considered as the outer and inner layers. So, increasing index p grows aluminum effect on the natural frequencies which has lower rigidity respect to the alumina.

δ_1	Method	Power law index (p)					
		0	0.2	0.5	1	2	∞
5	Present (FSDTS)	42.6836	39.0198	35.0369	30.9816	27.5790	19.4216
	Present (TSDTS)	42.6178	39.0006	35.0093	30.9850	27.5262	19.4019
	3D-DQM [Kiani et al. 2012]	42.6765	39.0419	35.0640	31.0262	27.5544	19.3003
10	Present (FSDTS)	42.3204	38.6806	34.7216	30.7226	27.3377	19.2585
	Present (TSDTS)	42.2793	38.6531	34.7061	30.6982	27.2765	19.2406
	3D-DQM [Kiani et al. 2012]	42.3285	38.7156	34.7591	30.7471	27.3169	19.1429

Table 3: Comparison of non-dimensional fundamental frequency parameters $\bar{\bar{\beta}} = \omega a \sqrt{\rho_m h / D_m}$ for SSSS Al/Al_2O_3 ($\rho_c = 3000\, kg/m^3$) doubly curved shell panels ($\tau = 0.1$, $\eta = 1$, $\delta_2 = \infty$ and $D_m = E_m h^3 / (12(1-\nu^2))$).

3.2 Effect of Side Ratio δ on the Fundamental Natural Frequency

Variations of fundamental natural frequency parameter β against side ratio changes are plotted in Figure 2. A FG square doubly curved panel with material properties as Al / Al_2O_3 and geometrical properties as $\tau = 0.15, 0.25, p = 1$ are considered. Figures are plotted for three boundary conditions

as SCSC, SSSS, and SFSF. Figures 2a and b show that increasing side ratio δ_1 reduces fundamental natural frequency. But Figure 2c shows reverse behavior which increasing side ratio δ_1 raises fundamental natural frequency. Also, increasing side ratio δ_1 and δ_2 has similar effect on the fundamental natural frequency. This is attributed to the fact that the geometrical (essential) boundary conditions such as the displacements *u, v, w* and the slopes ψ_1 and ψ_2, which are applied in the simply-supported and clamped edges, have direct relation with the curvature of the panel. So, increasing the side ratios δ_1 which decreases curvature of the panel reduces effect of geometrical boundary conditions. Indeed, geometrical boundary conditions have significant influences on the vibration of the doubly curved shell panel respect to the natural boundary conditions such as the stress resultants N_i , M_i *(i*=1,2,6*)* and Q_i *(i*=1,2*)*.

In addition, Figures 2a and b show that increasing thickness ratio τ reduces effect of side ratio increment on the fundamental natural frequency. In this case, increasing the thickness ratio τ reduce effect of curvature on the natural frequency. So, for thicker panels, changing side ratios δ_2 has not significant effect on the fundamental natural frequency.

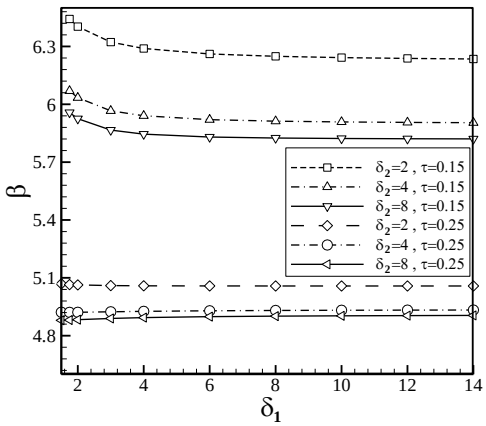

(a)

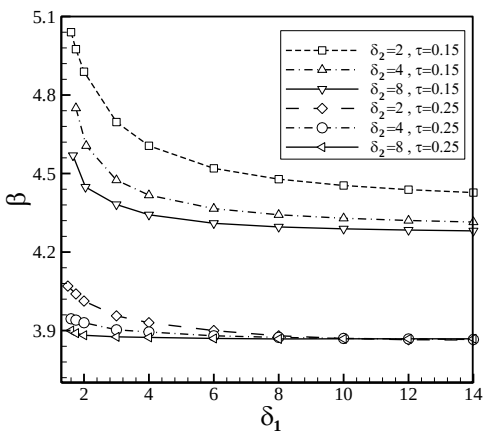

(b)

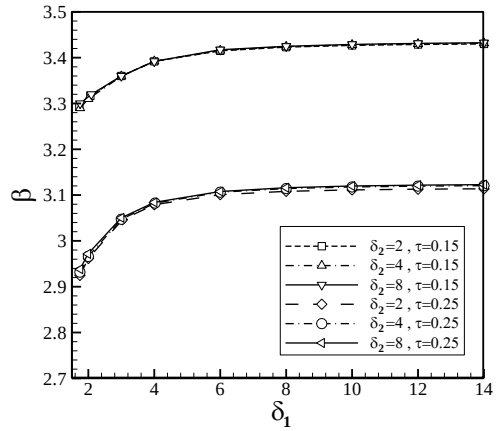

(c)

Figure 2: Variation of the fundamental frequency parameters β of Al/Al_2O_3 square doubly curved shell panel against radius to side ratios δ_1 and δ_2 for (a) SCSC (b) SSSS (c) SFSF boundary conditions when $\tau = 0.15, 0.25$ and $p = 1$.

3.3 Effect of Aspect Ratio η on the Fundamental Natural Frequency

Figure 3 shows effect of aspect ratio η on the fundamental natural frequency parameter of FG doubly curved panel. This effect is studied for three boundary conditions as SCSC, SSSS, SFSF and two material compositions as Al/Al_2O_3 and $Al/\mathrm{Zr}O_2$. By increasing aspect ratio η, panel transforms into strip which edges with simply-supported conditions place on longer side of strip. So, as shown in Figure 3a, increasing aspect ratio decreases effect of clamped edges which it reduce natural frequency. Also, in Figure 3b, increasing aspect ratio increases flexibility which it reduce natural frequency. But in Figure 3c, natural frequency increases because increasing aspect ratio increases ratio between lengths of simply-supported and free edges. Therefore, effect of aspect ratio on the panel rigidity and natural frequency depends on type of boundary conditions applied in the edges.

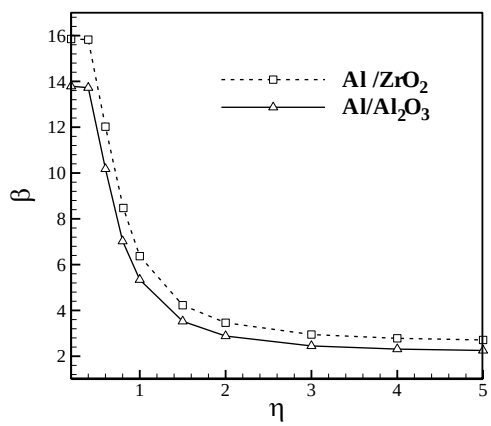

(a)

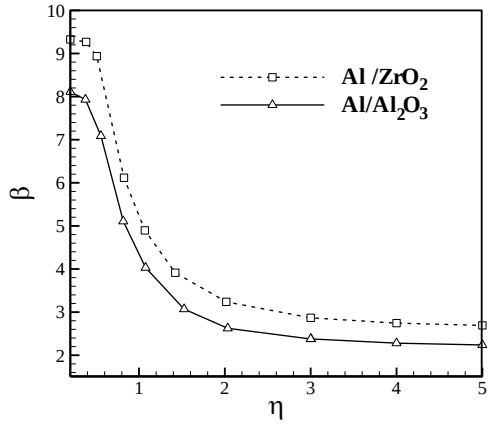

(b)

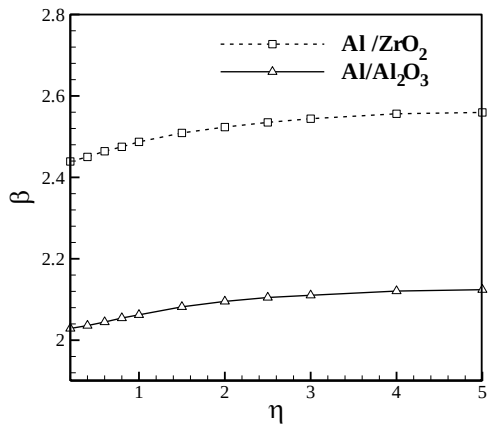

(c)

Figure 3: Variation of the fundamental frequency parameters β of Al/Al_2O_3 and $Al/\mathrm{Zr}O_2$ doubly curved shell panels against aspect ratios η for (a) SCSC (b) SSSS (c) SFSF boundary conditions when $\tau = 0.2$, $\delta_1 = 5$, $\delta_2 = 10$ and $p = 1$.

3.4 Effect of power law index *p* on natural frequency

Figure 4 shows effect of power law index p on the first and second fundamental natural frequencies parameters β for a square FG doubly curved panel. Two material properties and three boundary conditions are considered as indicated in figures. It can be concluded for figure 4 that increasing power law index decreases natural frequencies for such material compositions, generally. Variations start from frequencies of an isotropic material such as aluminum and reach to frequencies of an isotropic material with properties of Al/Al_2O_3 and $Al/\mathrm{Zr}O_2$. Furthermore, frequency variations against power law index are sharper for lower values than higher values.

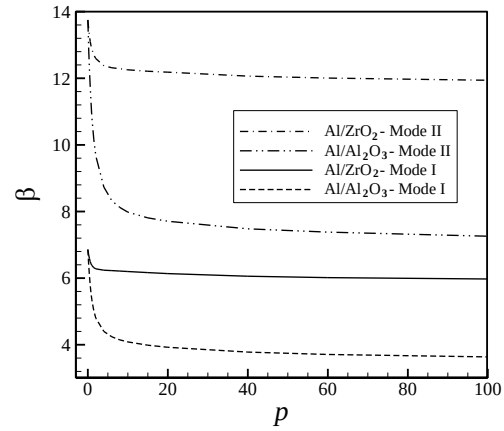

(a)

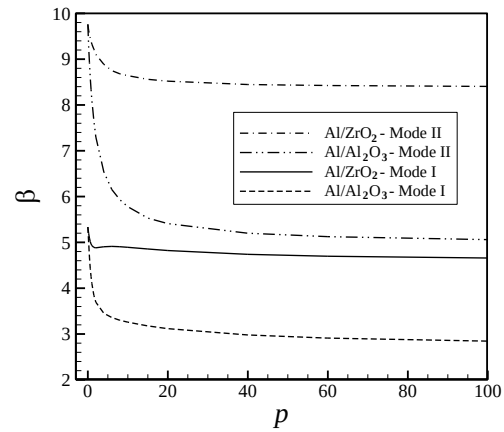

(b)

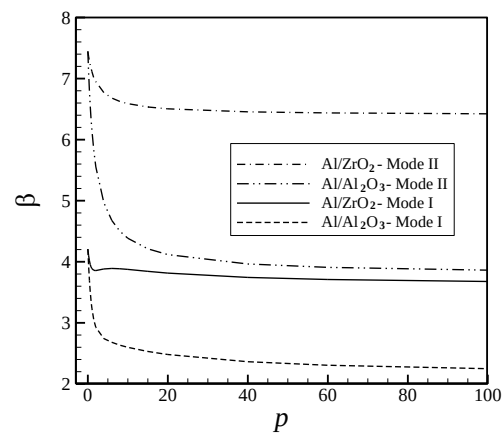

(c)

Figure 4: Effect of the power law index p on the first and second modes of FG square doubly curved shell panel for (a) SCSC (b) SSSS (c) SFSF boundary conditions when $\tau = 0.2$, $\delta_1 = 4$, $\delta_2 = 8$.

4 CONCLUSIONS

According to the Donnell and Sanders third order shear deformation type theories, a new exact close-form solution is presented to analyze free vibration of functionally graded doubly curved panel with Levy-type boundary condition. Validity and accuracy of the present method are confirmed by comparing its results with literature and finite element results. It is observed that Sanders theory has more accuracy respect to the Donnell theory. Also, effects of various geometrical and material parameters such as thickness, aspect ratio, and side ratio on natural frequency of FG panel are investigated. It is observed that effects of side ratio and aspect ratio on natural frequency depend on type of boundary conditions of the edges. In addition, it is shown that effect of power law index on natural frequencies is dependent to the material composition in the inner and outer layer of FG panel.

References

Akgöz, B., Civalek, Ö. (2013). Longitudinal vibration analysis of strain gradient bars made of functionally graded materials (FGM). Composites Part B 55: 263-268.

Alibeigloo, A., Chen, W.Q. (2010). Elasticity solution for an FGM cylindrical panel integrated with piezoelectric layers. Eur. J. Mech. A. Solids 29: 714-723.

Biglari, H., Jafari, A.A. (2010). High-order free vibrations of doubly-curved sandwich panels with flexible core based on a refined three-layered theory. Compos. Struct. 92: 2685-2694.

Chaudhuri, R.A., Kabir, H.R.H. (2005). Effect of boundary constraint on the frequency response of moderately thick doubly curved cross-ply panels using mixed fourier solution functions. J. Sound Vib. 283: 263-293.

Civalek, Ö. (2005). Geometrically nonlinear dynamic analysis of doubly curved isotropic shells resting on elastic foundation by a combination of harmonic differential quadrature-finite difference methods. Int. J. Press. Vessels Pip. 82: 470-479.

Donnell, L.H. (1934). A new theory for the buckling of thin cylinders under axial compression and bending. Trans. ASME 56: 795-806.

Farid, M., Zahedinejad, P., Malekzadeh, P. (2010). Three-dimensional temperature dependent free vibration analysis of functionally graded material curved panels resting on two-parameter elastic foundation using a hybrid semi-analytic, differential quadrature method. Mater. Des. 31: 2-13.

Fazzolari, F.A., Carrera, E. (2013). Advances in the Ritz formulation for free vibration response of doubly-curved anisotropic laminated composite shallow and deep shells. Compos. Struct. 101: 111-128.

Flügge, W. (1962). Statik und dynamik der schalen. Springer.

Hirai, T., Hirano, T., Kuroishi, N., Niino, M., Suzuki, A., Watanabe, R. (1988). Method of producing a functionally gradient material. Google Patents.

Hosseini-Hashemi, S., Ilkhani, M.R., Fadaee, M. (2012). Identification of the validity range of Donnell and Sanders shell theories using an exact vibration analysis of functionally graded thick cylindrical shell panel. Acta mech 223: 1101-1118.

Kiani, Y., Akbarzadeh, A.H., Chen, Z.T., Eslami, M.R. (2012). Static and dynamic analysis of an FGM doubly curved panel resting on the Pasternak-type elastic foundation. Compos. Struct. 94: 2474-2484.

Kiani, Y., Sadighi, M., Eslami, M.R. (2013). Dynamic analysis and active control of smart doubly curved FGM panels. Compos. Struct. 102: 205-216.

Lei, Z.X., Zhang, L.W., Liew, K.M., Yu, J.L. (2014). Dynamic stability analysis of carbon nanotube-reinforced functionally graded cylindrical panels using the element-free kp-Ritz method. Compos. Struct. 113: 328-338.

Liew, K.M., Lei, Z.X., Yu, J.L., Zhang, L.W. (2014). Postbuckling of carbon nanotube-reinforced functionally graded cylindrical panels under axial compression using a meshless approach. Comput. Meth. Appl. Mech. Eng. 268: 1-17.

Liew, K.M., Zhao, X., Ferreira, A.J.M. (2011). A review of meshless methods for laminated and functionally graded plates and shells. Compos. Struct. 93: 2031-2041.

Love, A.E.H. (1927). A treatise on the mathematical theory of elasticity. Cambridge University Press.

Messina, A. (2003). Free vibrations of multilayered doubly curved shells based on a mixed variational approach and global piecewise-smooth functions. Int. J. Solids Struct. 40: 3069-3088.

Mindlin, R. (1951). Influence of rotary inertia and shear on flexural motions of isotropic, elastic plates. J. of Appl. Mech. 18: 31-38.

Novozhilov, V.V. (1959). Thin shell theory. P. Noordhoff.

Reddy, J., Liu, C. (1985). A higher-order shear deformation theory of laminated elastic shells. Int. J. Eng. Sci. 23: 319-330.

Reddy, J.N. (2004). Mechanics of laminated composite plates and shells: theory and analysis. CRC press.

Redekop, D. (2006). Three-dimensional free vibration analysis of inhomogeneous thick orthotropic shells of revolution using differential quadrature. J. Sound Vib. 291: 1029-1040.

Reissner, E. (1945). The effect of transverse shear deformation on the bending of elastic plates. J. appl. Mech 12: 69-77.

Sanders Jr, J.L. (1959). An improved first-approximation theory for thin shells.

Sayyaadi, H., Askari Farsangi, M.A. (2014). An analytical solution for dynamic behavior of thick doubly curved functionally graded smart panels. Compos. Struct. 107: 88-102.

Singh, A.V. (1999). Free vibration analysis of deep doubly curved sandwich panels. Comput struct 73: 385-394.

Su, Z., Jin, G., Ye, T. (2014). Free vibration analysis of moderately thick functionally graded open shells with general boundary conditions. Compos. Struct.

Tornabene, F. (2009). Free vibration analysis of functionally graded conical, cylindrical shell and annular plate structures with a four-parameter power-law distribution. Comput. Meth. Appl. Mech. Eng. 198: 2911-2935.

Tornabene, F. (2011a). 2-D GDQ solution for free vibrations of anisotropic doubly-curved shells and panels of revolution. Compos. Struct. 93: 1854-1876.

Tornabene, F. (2011b). Free vibrations of anisotropic doubly-curved shells and panels of revolution with a free-form meridian resting on Winkler–Pasternak elastic foundations. Compos. Struct. 94: 186-206.

Tornabene, F., Fantuzzi, N., Bacciocchi, M. (2014). The local GDQ method applied to general higher-order theories of doubly-curved laminated composite shells and panels: The free vibration analysis. Compos. Struct. 116: 637-660.

Tornabene, F., Liverani, A., Caligiana, G. (2012). General anisotropic doubly-curved shell theory: A differential quadrature solution for free vibrations of shells and panels of revolution with a free-form meridian. J. Sound Vib. 331: 4848-4869.

Tornabene, F., Viola, E., Fantuzzi, N. (2013). General higher-order equivalent single layer theory for free vibrations of doubly-curved laminated composite shells and panels. Compos. Struct. 104: 94-117.

Vel, S.S. (2010). Exact elasticity solution for the vibration of functionally graded anisotropic cylindrical shells. Compos. Struct. 92: 2712-2727.

Viola, E., Tornabene, F., Fantuzzi, N. (2013). General higher-order shear deformation theories for the free vibration analysis of completely doubly-curved laminated shells and panels. Compos. Struct. 95: 639-666.

Wu, C.-P., Tarn, J.-Q., Tang, S.-C. (1998). A refined asymptotic theory for dynamic analysis of doubly curved laminated shells. Int. J. Solids Struct. 35: 1953-1979.

Zahedinejad, P., Malekzadeh, P., Farid, M., Karami, G. (2010). A semi-analytical three-dimensional free vibration analysis of functionally graded curved panels. Int. J. Press. Vessels Pip. 87: 470-480.

Zhang, L.W., Lei, Z.X., Liew, K.M., Yu, J.L. (2014a). Large deflection geometrically nonlinear analysis of carbon nanotube-reinforced functionally graded cylindrical panels. Comput. Meth. Appl. Mech. Eng. 273: 1-18.

Zhang, L.W., Lei, Z.X., Liew, K.M., Yu, J.L. (2014b). Static and dynamic of carbon nanotube reinforced functionally graded cylindrical panels. Compos. Struct. 111: 205-212.

Zhang, L.W., Zhu, P., Liew, K.M. (2014c). Thermal buckling of functionally graded plates using a local Kriging meshless method. Compos. Struct. 108: 472-492.

Zhu, P., Zhang, L.W., Liew, K.M. (2014). Geometrically nonlinear thermomechanical analysis of moderately thick functionally graded plates using a local Petrov–Galerkin approach with moving Kriging interpolation. Compos. Struct. 107: 298-314.

Hosseini-Hashemi, S., Fadaee, M. (2011). On the free vibration of moderately thick spherical shell panel—A new exact closed-form procedure. J Sound Vib 330 (17):4352-4367.